minerals

MDPI

Article

The Role of Water Content and Binder to Aggregate Ratio on the Performance of Metakaolin-Based Geopolymer Mortars

Felix Dathe [1,*], Steffen Overmann [2], Andreas Koenig [3,†] and Frank Dehn [1,†]

[1] Institute of Concrete Structures and Building Materials, Karlsruhe Institute of Technology (KIT), Gotthard-Franz-Str. 3, 76131 Karlsruhe, Germany; frank.dehn@kit.edu
[2] Institute of Building Materials Research, RWTH Aachen University, Schinkelstr. 3, 52062 Aachen, Germany; overmann@ibac.rwth-aachen.de
[3] Department of Prosthodontics and Material Sciences, Leipzig University, Liebigstraße 12, 04103 Leipzig, Germany; akoenig@uni-leipzig.de
* Correspondence: felix.dathe@kit.edu
† These authors contributed equally to this work.

Abstract: Geopolymers are in many applications a perfect alternative to standard cements, especially regarding the sustainable development of green building materials. This experimental study therefore deals with the investigation of different factors, such as the water content and the binder to aggregate ratio, and their influence on the workability of fresh mortar and its mechanical properties and porosity on different size scales. Although increasing the water content improved the workability and flow behaviour of the fresh mortar, at the same time, a reduction in compressive strength in particular and a lesser reduction in flexural strength could be demonstrated. This finding can be attributed to an increase in capillary porosity, as demonstrated by capillary water uptake and mercury intrusion porosimetry measurements. At the same time, the increasing water content led to an improved deaeration effect (low air void content) and to initial segregation (see the µXCT measurements). An alternative approach to enhance the compressive and flexural strengths of the mortar specimens is optimization of the binder to aggregate ratio from 1 to 0.25. This study paves the way for a comprehensive understanding of the underlying chemistry of the geopolymerization reaction and is crucial for the development of sustainable alternatives to cementitious systems.

Keywords: geopolymers; CO_2 reduction; common clays; capillary porosity; geopolymerization; alkali activation; metakaolin

Citation: Dathe, F.; Overmann, S.; Koenig, A.; Dehn, F. The Role of Water Content and Binder to Aggregate Ratio on the Performance of Metakaolin-Based Geopolymer Mortars. *Minerals* **2024**, *14*, 823. https://doi.org/10.3390/min14080823

Academic Editors: Dariusz Mierzwiński, Wei-Ting Lin and Paulina Faria

Received: 20 June 2024
Revised: 2 August 2024
Accepted: 10 August 2024
Published: 14 August 2024

1. Introduction

According to the International Energy Agency (IEA) and the United Nations Environment Program (UNEP), the construction area contributes to more than 40% of the energy consumption worldwide and about a third of greenhouse gas emissions [1]. In this context, the production of concrete represents a significant environmental burden, since about 5 to 7% of anthropogenic CO_2 emissions come from global concrete production [2]. For the production of every ton of Portland cement about 1.5 tons of raw materials are needed, while about one ton of CO_2 is released [3]. These numbers are rising every year due to an increased demand for construction materials. The immense amounts of raw materials needed and the high level of CO_2 emissions make cement production extremely resource and energy intensive.

In order to ensure a sustainable development of the construction sector, alternatives to conventional cementitious binders with a low carbon footprint have to be found. In this context, geopolymers have attracted more and more attention [4]. The term geopolymer was established by Davidovits in 1978 and refers to binder materials based on alkali-activated alumosilicates [5,6]. Geopolymers can be obtained from a polymerization reaction of an

alumosilicate material in the presence of an alkaline solution, such as sodium hydroxide, sodium silicate, potassium hydroxide or potassium silicate, as an activator (Figure 1).

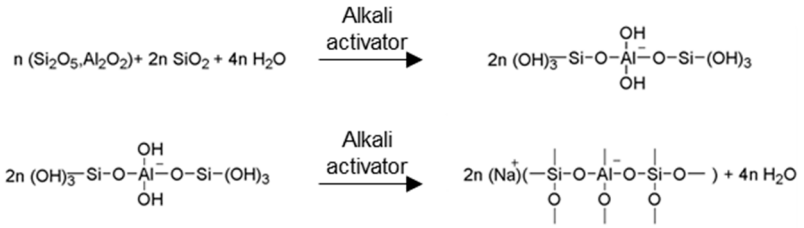

Figure 1. Geopolymerization reaction according to Davidovits [5].

As a starting material for the production of the geopolymer metakaolin, slag or alumosiliceous fly ash are commonly used [7,8]. Metakaolin is a dehydroxylated form of the clay mineral kaolinite and its structure is based on an amorphous (non-crystalline) aluminosilicate network, which can be activated by a base to form a corresponding geopolymer. Recently, also common clays, as widely occurring and cheap resources, have been investigated as raw materials for geopolymer production [9–13]. Such alternative binders based on sustainable resources are also being referred to as "Green Concrete" [14]. In addition to improved sustainability, these mortars/concretes have improved resistance to chemical agents (acids, sulfates) or high temperatures due to their alumosilicate network [15–17].

Despite the fact that geopolymers have been known for almost 50 years, the geopolymerization reaction is not completely understood. It is a very complex reaction that depends on many experimental factors. Consequently, a targeted mixing design to afford defined geopolymers with predictable properties, such as workability or tensile and compressive strengths, is challenging. To overcome this, attempts to rationalize the experimental parameters for the mixing design of metakaolin-based geopolymers, such as the sodium silicate to sodium hydroxide ratio and the alkaline solids to metakaolin ratio, were, for example, reported by Al-Salloum et al. Thereby, it was shown that the workability of the fresh mortars improved with an increased sodium silicate to NaOH ratio until a certain limit, while also the compressive strength was found to be increased [18]. In this context, it was also shown that by using a higher NaOH concentration during the activation, the polymerization degree within the mortar specimens could be increased [19]. The compressive strength of geopolymers was also reported to be improved through the addition of waste, such as pent abrasive powder, which was mainly composed of corundum grains [20]. Down this road, also the addition of dyes, such as bromothymol blue, cresol red, phenolphthalein, and methyl orange, to the geopolymer mixture has been described with the aim to provide colored geopolymers, which are suitable for design and restoration applications. Thereby, it was found that the fresh mortars exhibited a good workability, while there was no significant change in the microstructural 3D network of the geopolymer mortars observed [21].

Apart from these factors, the water content of the mixture and the associated solid to liquid ratio is also crucial, since it not only influences the fresh mortar properties but also the mechanical properties of the final mortar specimens [12]. Water is not only the reaction medium in which the dissolution of the raw materials and the ions takes place but also an integral part of the polymerization reaction itself, since it takes part in the hydrolysis and polycondensation of Al- and Si-containing oligomers [20]. In addition, water has a major influence on the workability of the fresh mortar. As the thickness of the water film on the particles increases, the internal friction is reduced, which results in increased flowability of the fresh mortar. Beside the positive effect of water in the context of the geopolymer formation, it has been reported that the addition of water and the associated reduction in alkalinity of the reaction system [21] can lead to a migration of ions away from the reaction zone. Also, an excess of water might influence the chemical equilibrium of the geopolymerization reaction according to the principle of Le Chatelier and push the equilibrium to the side of the starting materials, which leads to a reduction in

the polymerization rate [22]. This is complicated by the fact that the water is chemically bound to a lesser extent in the geopolymerization process compared to common cement hydration. This leads to the assumption that the porosity in the hardened geopolymer mortar/concrete is more clearly influenced by the water content. Therefore, the addition of water is a balancing act for the successful preparation of geopolymers via alkali solutions.

Although the role of water was investigated in some papers [14,20,23–25], no comprehensive studies using advanced analytic techniques, such as micro X-ray computer tomography, were carried out. In this paper, we therefore studied the alkali activation of metakaolin with the aim of finding a suitable water content and consequently an optimal formulation for the geopolymerization of calcined clay to produce geopolymer-based mortars with low porosity and high compressive as well as tensile flexural strengths. In this context, we also examined the binder to aggregate ratio in detail using various analytic techniques, such as X-ray powder diffraction (XRD), mercury intrusion porosimetry (MIP), and micro X-ray computer tomography (μXCT). This fundamental understanding of the geopolymer chemistry and the rationalization of the factors that can influence the geopolymerization reaction is crucial for the sustainable production of green building materials.

2. Materials and Methods

2.1. Raw Materials

Metakaolin (Metamax®) was purchased from BASF (Ludwigshafen, Germany), while the aqueous NaOH solution (50 wt.% NaOH) was obtained from Carl Roth GmbH & Co. KG (Karlsruhe, Germany). A sodium silicate solution (Betol39T®) from Woellner GmbH (Ludwigshafen, Germany) with a concentration of 34.5 wt.% and a SiO_2 to Na_2O molar ratio of 3.4 was used. Either quartz powder (MILLISIL W3®, Quarzwerke GmbH, Frechen, Germany) or CEN standard sand (0.08–2 mm) according to DIN EN 196-1:2016-11 were used as inert aggregates. The powder X-ray diffractograms of Metamax® and MILLISIL W3® are shown in the Supplementary Material (Figures S1 and S2).

2.2. Sample Preparation

All experiments were carried out under controlled laboratory conditions at 20 °C and 50% relative humidity. The manufacture and casting of the mortar specimens was carried out according to a modified DIN EN 196-1:2016-11 procedure [26]. Based on previous experiments and the successful formation of suitable geopolymer mortars [11], 450 g metakaolin powder was added to 225 g of an aqueous sodium silicate solution. While the mixture was stirred, aqueous sodium hydroxide solution (50 wt.%, 450 g) and water (according to the mixing designs shown in Tables 1 and 2) were added. The corresponding molar ratios are shown in the Supplementary Material (Table S2). Subsequently, CEN standard sand was added to the mixture while stirring. For the investigation of the influence of the binder to aggregate ratio on the workability of the fresh mortar and the strength of the mortar specimens, quartz powder was added as aggregate instead of CEN standard sand. The metakaolin/quartz powder ratio was varied from 100/0 to 20/80. The resulting mortars were then cast in standard prisms ($40 \times 40 \times 160$ mm^3) for the investigation of the influence of water or prisms of $20 \times 20 \times 80$ mm^3 for the investigation of the aggregate addition. The smaller prism size of the latter enabled a timely analysis of a large number of specimens. All samples were demolded 24 h after casting and stored wrapped in foil. The storing of the samples took place under controlled conditions (65% relative humidity and 20 °C) until further tests were carried out.

Table 1. Mixing design for the geopolymers mortars. W/S refers to the water to solid content of the fresh lime and the mortars, to which sand was added.

Code	Additional Water in g	W/S (Fresh Lime)	W/S (Mortar)
GP_Ref	0	0.57	0.20
GP_50	50	0.64	0.22
GP_100	100	0.71	0.25
GP_150	150	0.78	0.27

Table 2. Mixing design for the alkali activation of metakaolin and quartz powder (in g).

Code	Metakaolin	Quartz Powder	Sodium Silicate	50 wt.% NaOH	H_2O from Sodium Silicate and NaOH
GP_100/0	500	0	500	250	445.0
GP_90/10	450	50	450	225	400.5
GP_80/20	400	100	400	200	356.0
GP_70/30	350	150	350	175	311.5
GP_60/40	240	160	240	120	213.6
GP_50/50	200	200	200	100	178.0
GP_40/60	160	240	160	80	142.4
GP_30/70	120	280	120	60	106.8
GP_20/80	80	320	80	40	71.2
GP_20/80 + 20 g H_2O	80	320	80	40	91.2

2.3. Methods

For the powder X-ray diffraction analyses, a D8 Advance Bruker diffractometer with a Lynxeye Detector (Bruker, Ettlingen, Germany) was used. Experiments were carried out with Copper Kα radiation in a 2θ area between 5° and 70° in 0.02° steps with a scanning time of 0.2 s. The powder X-ray diffractograms of the precursor materials (metakaolin and quartz powder) and the mortar specimens (GP_Ref and GP_150) are shown in the Supplementary Material (Figures S1, S2 and S7). The light microscopic determination of the air void content was carried out on polished mortar samples with an Olympus SZX 10 microscope according to DIN EN 480-11:2005-12 [27]. The pore size distributions of all mortar specimens (GP_Ref, GP_50, GP_100, GP_150) according to incident light microscopy are shown in the Supplementary Material (Figure S3). A micro X-ray computer tomograph with a directional X-ray tube FXE 225.99 ($\leq$225 kV, focal spot diameter $\leq$3 mm, tungsten target) by YXLON International GmbH (Hamburg, Germany) and a 2D-detector 1621xN (2.048 × 2.048 pixels, CsI, pitch size 200 × 200 µm^2) by PerkinElmer (Waltham, MA, USA) were used to determine the macro pores and the grain distribution in the GP_Ref, GP_50, GP_100, GP_150 samples (Figure 5 and Figure 6). Measurements were carried out on drill cores of the diameter d = 6.5 mm and height h = 40 mm, which were extracted from the mortar specimens. The macro pore distribution analysis of the experimental data was carried out with software ImageJ 1.47v (National Institute of Health, Bethesda, MD, USA) and VG Studio Max 2.0v (Volume Graphics GmbH, Hamburg, Germany) based on [28]. For the SEM images, a LEO 1530 Gemini Carl Zeiss microscope with a secondary electron detector was applied to investigate the polished and unpolished fragments within the GP_Ref, GP_50, GP_100, and GP_150 samples (Figure 7). For the water absorption measurements, a cube with an edge length of 40 mm of each sample was dried until a mass constancy was reached (24 h, 105 °C). Afterward, the dried cubes were placed in a vessel with 400 mL of water and weighed after 4 h and 24 h to confirm a constant mass of the cubes, which results in a complete saturation of the mortar specimens (GP_Ref, GP_50, GP_100, GP_150) with water to detect open pores. The results are depicted in Figure 3, and based on these experiments, the pores filled with water can be calculated and the water absorption dependent porosities were obtained (Table 4) according to the following equation:

$$\varepsilon_w = \frac{(m_s - m_d)}{\rho_w * V} * 100$$

ε_w = porosity determined for water
m_s = mass of the water saturated specimens
m_d = mass of dried specimens
p_w = density of water
V = sample volume

Nitrogen adsorption measurements of GP_Ref were carried out using a NOVA Touch LX1 provided by Quantachrome under liquid nitrogen cooling to determine the specific surface of the pores with a diameter between 0.35 to 400 nm (Supplementary Material, Figures S4 and S5). For the determination of the pore size distribution of GP_Ref, GP_50, GP_100, and GP_150 via mercury intrusion porosimetry, a Pascal 440 device from Thermo Fisher Scientific was used (Figure 4, Supplementary Material, Figure S6). The additional module 140 (low pressure) could cover the pore radii between 3.6 and 100,000 nm. The measurement was performed on fragments. The compressive and flexural strengths of all mortar specimens, in standard prisms (40 × 40 × 160 mm^3) for the investigation of the influence of water or prisms of 20 × 20 × 80 mm^3 size for the investigation of the aggregate addition, were determined seven days after their manufacture with a RT 200/10-1s device of the company Testing Bluhm & Feuerherdt according to DIN EN 196-1:2016-11 [26]. The applied loading rate for the determination of the compressive strength was 2400 N/s, whereas a loading rate of 50 N/s was used for the flexural strength. The results are depicted in Figure 9 and Figure 10 as well as in the Supplementary Material (Table S1). The workability of the fresh mortars (GP_Ref, GP_50, GP_100, GP_150) was tested via a flow spread test on a flow table according to DIN EN 1015-3:2007-05 [29] (Table 3). Right after the mixing process, the fresh mortar was placed in a truncated cone (Ø 100 mm) on a Hägermann flow table. After 15 hits, the spread of the fresh mortar was measured in both directions and the average flow spread was calculated.

Table 3. Flow spread test results of the fresh mortars.

Code	Flow Spread in mm	Relative Flow Spread	Consistency
GP_Ref	190	2.6	Plastic mortar
GP_50	245	5.0	Soft mortar
GP_100	275	6.6	Soft mortar
GP_150	>300	8.0	Very soft mortar

3. Results and Discussion

3.1. The Role of the Water Content in the Geopolymerization Process

3.1.1. Workability of the Fresh Mortar

In order to evaluate the workability of the fresh mortar, flow spread tests were carried out after varying the water content of the samples. As shown in Table 3, the flow spread increased with an enhanced water content of the geopolymer mixture. This corresponds to an easier to handle mortar, which is beneficial for the subsequent casting process.

3.1.2. Investigation of the Porosity of Mortar Specimens

The porosity of the mortar specimens was investigated in detail using light-based imaging methods, the examination of the water absorption, low temperature adsorption of nitrogen, mercury intrusion porosimetry and scanning electron microscopy (Figure 2) [30]. In addition to these analytical techniques, we used micro X-ray computer tomography to image micro-structures in three dimensions and to determine the porosity of the mortar specimens [19]. The existence of micropores (pores < 2 nm) within the mortar specimens was ruled out by N_2 adsorption measurements, as shown in the Supplementary Material (Figures S4 and S5).

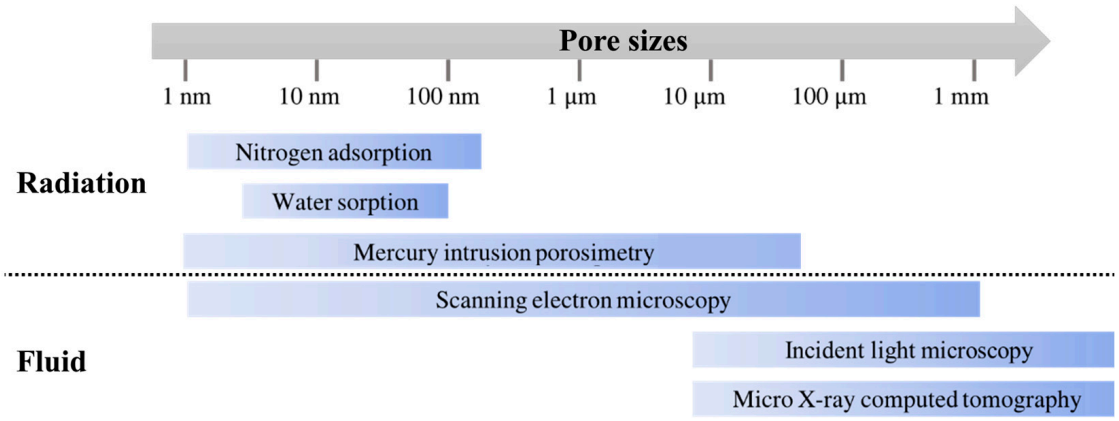

Figure 2. Relevant pore sizes and appropriate analytical methods for their determination.

The porosity of the mortar specimens was determined from the water absorption. During these experiments, the mass difference between dried mortar specimens and mortar specimens that were submerged in water was determined (Figure 3).

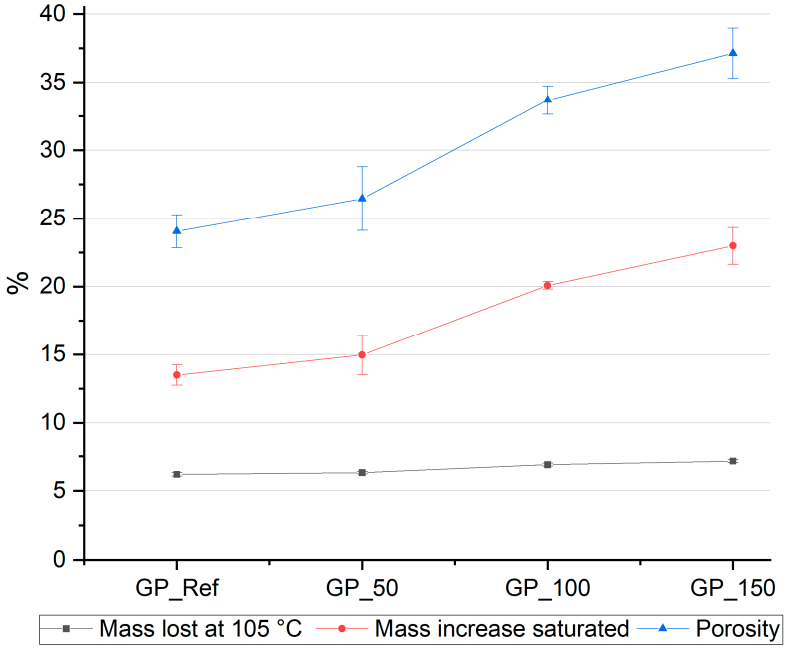

Figure 3. Determination of the water absorption and the porosity via drying and water uptake; mass loss at 105 °C to mass constancy (black); mass increase saturated (red); and calculated porosity (blue).

During the drying process, an almost linear mass loss of about 0.9% is witnessed with increasing water content of the geopolymer mixtures. After the drying process, fine cracks can be observed within the mortar specimens, which can be attributed to the shrinkage of the material and the different expansion coefficients of the various components. For the water uptake, again, an almost linear increase with increasing water content of the geopolymer mixture can be witnessed. The maximum difference amounts to 7.4% and is therefore about 10 times higher than the mass loss detected during the drying process.

Based on these experiments, the volume of the pores filled with water can be calculated and porosities between 24.05% and 35.8% were obtained. As it becomes obvious from Table 4, the porosity increased with increasing water content of the geopolymer mixture.

Table 4. Porosity determined via the investigation of the water absorption measurements.

Code	Porosity by Water Absorption in %
GP_Ref	24.05 ± 1.2
GP_50	26.5 ± 2.3
GP_100	33.7 ± 1.1
GP_150	37.1 ± 1.8

The meso- and macropores of the mortar specimens were analyzed by mercury intrusion porosimetry. The cumulative pore volume, the average pore diameter and the specific surface area obtained from mercury intrusion porosimetry are depicted in Figure 4. For these calculations based on the Washburn-equation [31], 3.050 nm was selected as the upper threshold (Supplementary Material, Figure S6).

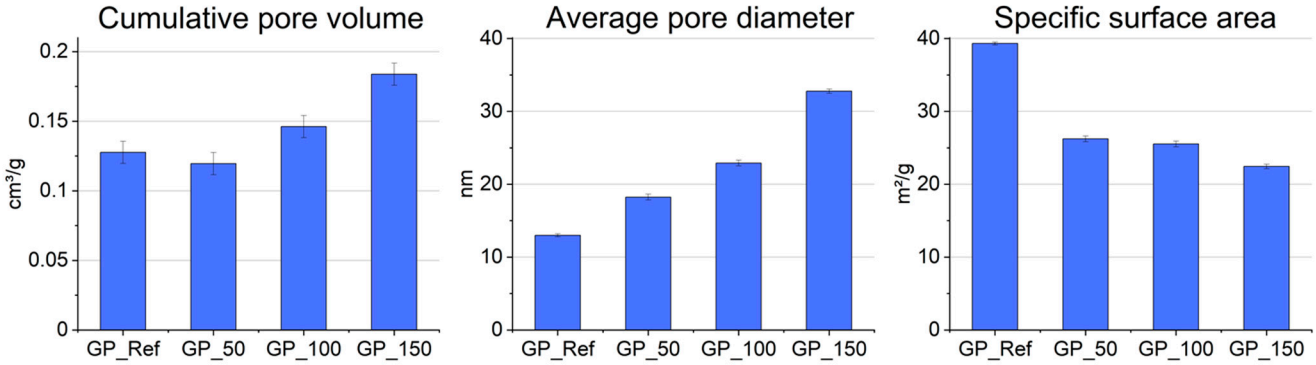

Figure 4. Results of the mercury intrusion porosimetry. Pore volumes are presented in cm^3/g of geopolymer with an error of ±0.008 cm^3, according to [32].

The cumulative pore volumes (Figure 4) and the resulting porosities (Table 5) show an almost linear increase with increasing water content. In cases of the average pore diameter, again, an increase can be witnessed when the water content in the geopolymer mixture is enhanced. While an enhancement of the average pore diameter with increasing water content was witnessed, the specific surface area decreased.

Table 5. Porosities of the mortar specimens determined via mercury intrusion porosimetry.

	Porosity in %	Cumulative Pore Volume in cm^3/g	Average Pore Diameter in nm
GP_Ref	24.2	0.128	13.0
GP_50	23.0	0.120	18.2
GP_100	26.8	0.146	22.9
GP_150	31.5	0.184	32.8

To gain structural information regarding the porosity in the size range of macro pores like air voids (Ø 0.020–10 mm), micro X-ray computer tomography (µXCT) measurements of the mortar specimens were carried out. Also, µXCT gives information about the distribution of the aggregated particles. With the used measurement setup, a resolution of 10 µm was achieved. The results of the µXCT of the drill cores for all mortar specimens are depicted in Figure 5.

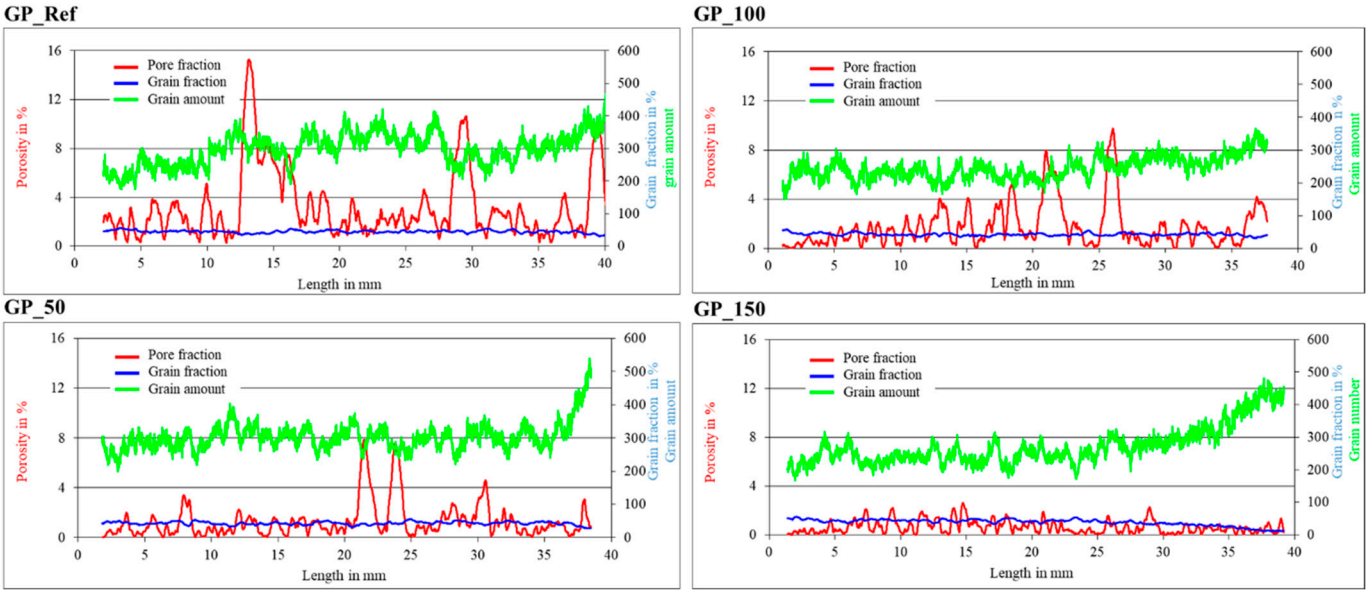

Figure 5. Pore and grain distribution through the cores of the mortar sample prisms obtained via µXCT measurements. The length of 0 mm corresponds to the bottom of the mortar sample prisms.

These results show that in the reference geopolymer mortar and in the mortars to which 50 g and 100 g of water were added, the grain fraction stays constant over the whole length of the drill core. However, the spatially resolved analysis of the drill core of the mortar, to which the highest amount of water (150 g) was added, shows a decrease of the grain fraction starting at a height of 30 mm. This is due to the low viscosity of the fresh mortar of GP_150, which leads to a gravity-related segregation of the grains and to the accumulation of the biggest grains within the bottom area of the drill core.

Obviously, not only the grain fraction is influenced by the water content of the mixture but also the porosity regarding air voids. It becomes clear that mixtures with a lower water content exhibit a higher amount of air voids than samples with a higher water content (Figure 6). A higher amount of air voids can be attributed to the high viscosity of the fresh mortar and the associated worse workability. Similar findings were made in the context of alkali-activated materials based on Sicilian volcanic precursors (i.e., volcanic ash and pumice), although here also the particle size of the applied precursors was shown to be a decisive factor in the porosity of the mortar specimens [33].

The observed porosity trend is inverse to the porosities determined via water absorption and mercury intrusion porosimetry since these techniques always indicated an increase in porosity with an enhanced water content. However, in the case of the µXCT measurements, only air voids that consist of 8 voxels were analyzed (Ø ~20 µm ≈ 8000 µm^3) and no smaller pores can be detected, which explains the different trends in comparison with the other analytical techniques. This finding is also supported by incident light measurements, where GP_Ref shows the highest number of pores over the whole size range as shown in the Supplementary Material (Figure S3).

The microstructures and porosities of the mortar specimens were investigated by scanning electron microscopy (Figure 7). From the images, a heterogeneous distribution of aggregates within the binder matrix becomes obvious. Also, cracks within the specimens can be witnessed, which most likely stem from the drying process. Similar microstructures have been reported for other metakaolin-based geopolymers [18].

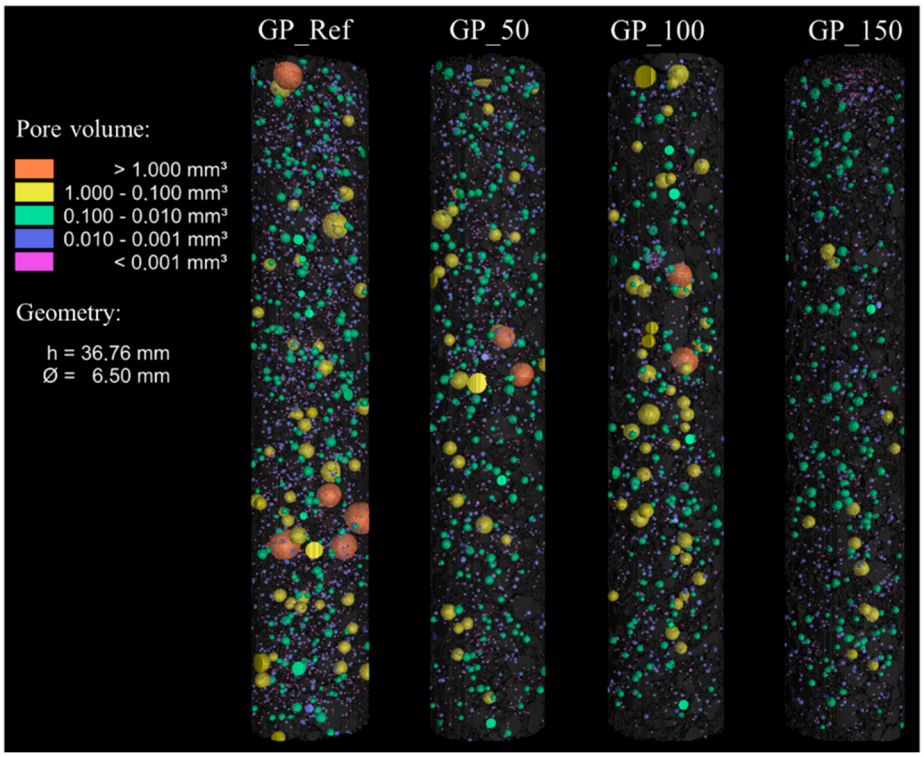

Figure 6. 3D representation of the pore size distribution within the drill core. The drill cores are oriented according to their casting direction, but cut off at about 1.6 mm.

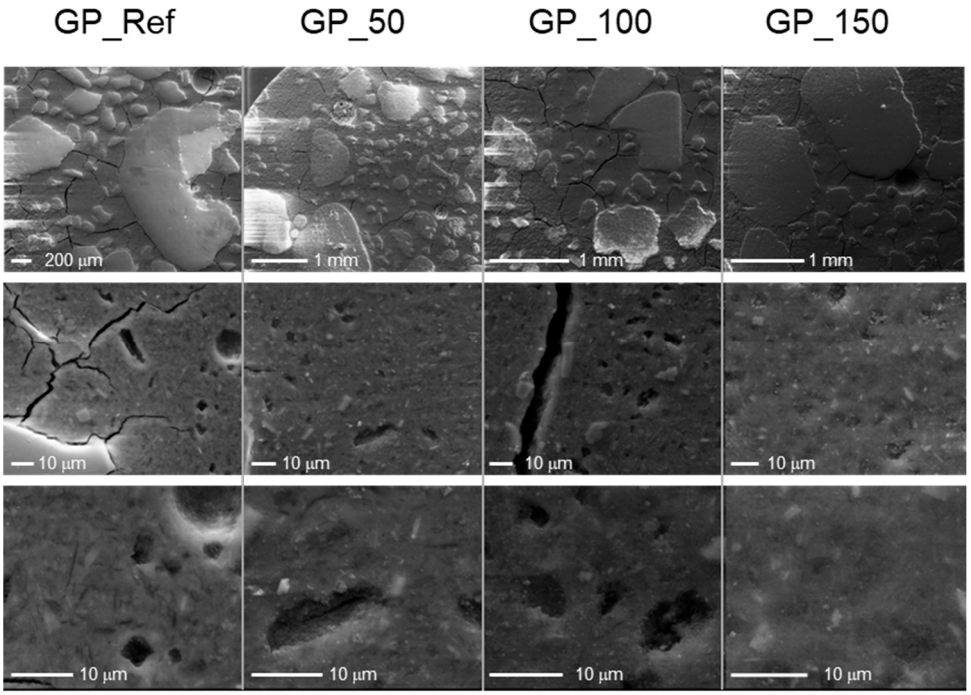

Figure 7. Scanning electron microscopy images of the mortar specimens. From left to right. GP_Ref, GP_50, GP_100, and GP_150. The resolution increases from the top to the bottom.

The mortar specimens GP_Ref and GP_150 were crushed and investigated by powder X-ray diffraction. In the resulting diffractogram (Figure 8), the crystalline phases of quartz, anatase, muscovite and albite can be identified. These phases belong to the aggregate used in the mortar. The geopolymer binder is amorphous and does not lead to any diffraction reflexes in the pattern. You can see clearly that the crystalline composition of GP_Ref and

GP_150 is identical. These results show us that the additional water does not lead to a change in crystallinity and the effect on porosity is due to other mechanisms.

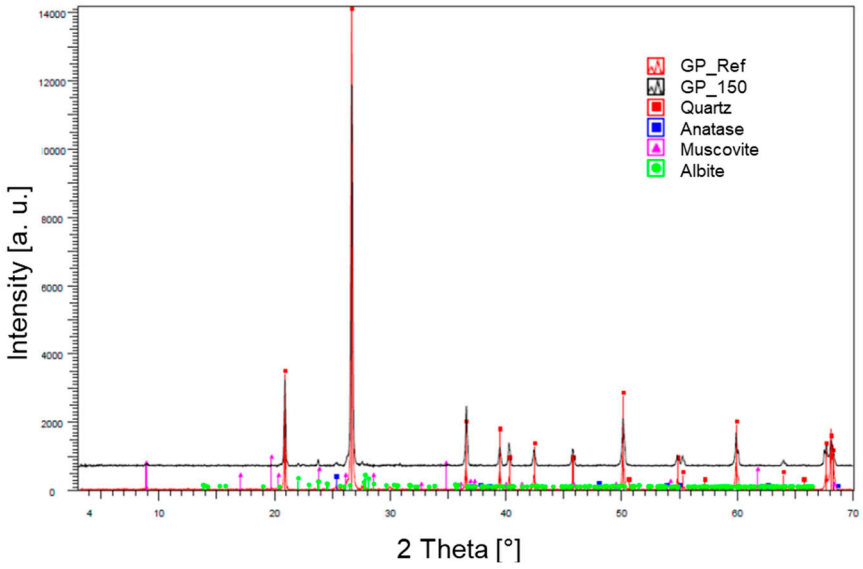

Figure 8. Powder X-ray diffraction of the mortar GP_Ref and GP_150.

3.1.3. Mechanical Properties of the Mortar Specimens

The compressive and flexural strengths of the mortar specimens were determined and it becomes obvious that a higher water content (w/s = 0.27 for mortar) leads to a reduction in the compressive strength (Figure 9). Consequently, the compressive strength is found to be inversely proportional to the water content of the geopolymer mixture, which is similar to observations made for the water-to-solid ratio in other metakaolin-based geopolymers [18] as well as for the water-to-cement ratio in conventional cementitious systems [34]. Similar observations were made for the tensile flexural strength of the mortar specimens. Only the reference mortar showed a slight deviation from this trend, but at the same time the highest standard deviation.

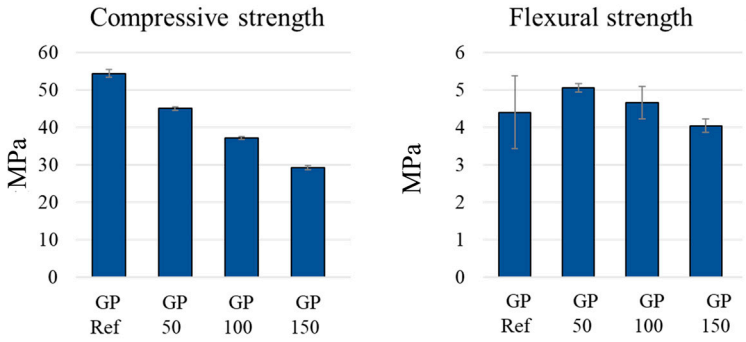

Figure 9. Compressive (6 values per mean value) and flexural (3 values per mean value) strengths with standard deviation of the mortar specimens.

The strength measurements clearly correlate with the porosities of the mortar specimens determined via capillary water uptake and mercury intrusion porosimetry measurements. It becomes obvious that a higher water content within the geopolymer mixture leads to an enhanced porosity of the mortar specimens, which results in a reduction of the compressive and flexural strengths. It is noticeable that the compressive strength decreases significantly more than the flexural strength due to the increasing water content. This behavior is unexpected. Normally, pores are usually compressed in compression testing and in flexural strength they have a reduced tensile cross-sectional area and a crack-initiating effect.

However, a low water content significantly reduces the workability of the fresh mortar, as the flow spread tests carried out have shown. Also, a low water content leads to a high amount of air voids, which were observed via micro X-ray computed tomography (Section 3.1.2 as well as incident light microscopy (see Supporting Information). Therefore, the macro pores have a lower influence than the smaller pores (<20 µm) on the mechanical performance. In order to produce geopolymers with good mechanical properties, the water content should be kept as low as possible.

3.2. The Role of the Binder to Aggregate Ratio

Although an increase in water content in a geopolymer mixture leads to a better workability of the mortar, a clear reduction in the compressive strength and a lesser reduction in the flexural strength was observed. Therefore, an alternative approach, namely the variation of the binder to aggregate ratio, was investigated with the aim of enhancing the workability of the mortar while good strengths of the mortar specimens are maintained. Whereas in the case of GP_Ref, GP,50, GP_100 and GP_150 a fixed amount of CEN sand (1350 g) was added as aggregate, in this section, a systematic study of the ratio variation of metakaolin and quartz powder as aggregate was carried out. In this case, quartz was selected as a non-reactive aggregate in powder form. In order to optimize the formulation of the geopolymer mortar, various binder to aggregate ratios varying between 1.0 and 0.25 were prepared.

Mechanical Properties of the Mortar Specimens

For the investigation of the effect of the quartz powder inclusion in the geopolymer mortars, the compressive and flexural strengths of the mortar specimens were determined depending on the binder to aggregate ratio (Figure 10). It becomes obvious that the geopolymerization of pure metakaolin without the addition of quartz powder results in mortar specimens with a compressive strength of 46.6 MPa and no detectible flexural strength. Very similar strength values were determined for the 90/10, 80/20 and 70/30 binder to aggregate mixtures. However, when the binder to aggregate ratio is reduced and the quartz powder content is increased, an enhancement of the compressive and flexural strengths can be witnessed. The maximum compressive strength of 81.4 MPa was achieved with a 20/80 binder to aggregate ratio. It is known from the development of ultra-high performance and eco-friendly concretes that the partial replacement of the reactive component (cement) by quartz powder can increase the packing density, due to the more finely tuned grain band, and thus the strength [27]. This physical mode of action can apparently be transferred for the metakaolin-based geopolymer since Li et al. demonstrated a similar increase in compressive strength (83/17 ratio) with a heat-treated metakaolin-based geopolymer. When 20 g of additional water is added to the 20/80 mixture, the compressive and flexural strength decrease. This is in complete accordance with the water content results shown before (Section 3.1).

These results are astonishing since the increase in aggregate ratio leads to an improvement of the compressive and flexural strengths of the mortar specimens within the investigated binder to aggregate ratio regime. Similar observations were made for geopolymer concrete made from alkali-activated fly ash, where an enhancement of the flexural strength of geopolymer concrete was observed with an increase in the total aggregate content [28]. Also, an increase in compressive strength has been observed for metakaolin-based geopolymers with a maximum at a 73.8% aggregate content. However, the reported compressive strengths were approximately 20 MPa below the compressive strength observed for the mortar specimens described in this study [18]. Consequently, these experimental findings can be considered as model experiments for the geopolymerization of common clays, since common clays can be considered as natural mixtures of aggregate with metakaolin, with a metakaolin content of below 50%.

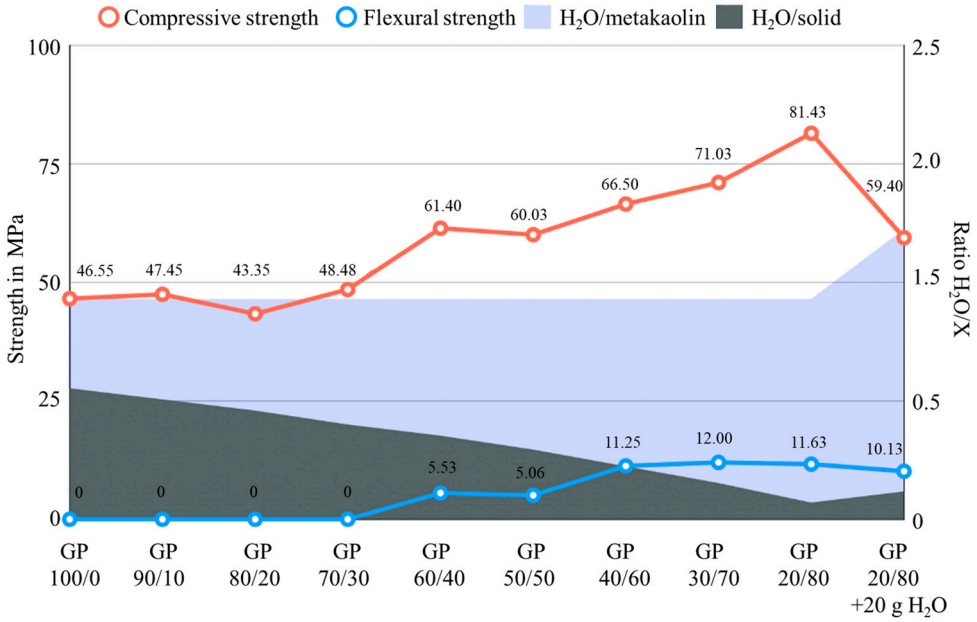

Figure 10. Compressive (six values per mean value) and flexural strengths (three values per mean value) of the mortar specimens depending on the metakaolin to quartz powder ratio.

The rationalization for this experimental observation is difficult, since the binder to aggregate interface within geopolymer binders is still poorly understood, especially at a molecular level. However, only recently, interfacial bonding including Al–O–Si, Na–O and H-bonding, was investigated using molecular dynamics simulations. The simulations have shown that the Si/Al ratio is crucial for the interfacial strength due to a higher degree of interaction and more cross-linking within the geopolymer [35]. In order to increase the interfacial bonding between aggregates and geopolymer binders, it has been shown that the presence of soluble silicates, as Betol39T® in the case of this study, in the initial activating solution is beneficial [36]. However, at this point, it must be mentioned that the experimental observations are highly dependent on the raw materials used for the geopolymer production [37,38]. Studies on the binder to aggregate ratio using high calcium fly ash together with sodium metasilicate as binder and sand as aggregate have, for example, shown an inverse effect, where a reduction of the strength with increasing aggregate proportion was observed [39]. Similar observations were made for the alkali activation of low grade kaolin [40].

4. Conclusions

Geopolymers have gained more and more attention when trying to find sustainable alternatives to hydraulic binders (e.g., normal cements based on Portland cement clinker), especially with respect to a desired reduction of greenhouse gas emissions. In this work, therefore, the influence of different factors, such as the water content and the binder to aggregate ratio, on the formation of geopolymer mortars were investigated with the aim of identifying an optimal mixing design. The main intention was hereby to combine a good workability of the fresh mortar with low porosity and high compressive as well as flexural strength of the resulting mortar specimens. To achieve this, we cast mortar specimens using different ratios of metakaolin and water ranging from water to solid contents of the fresh lime of 0.57 to 0.78. The porosity of these specimens was then evaluated by water absorption measurements, mercury intrusion porosimetry, micro X-ray computer tomography and scanning electron microscopy. Subsequently, the mechanical properties, such as the tensile and compressive strengths, of the mortars were determined. To investigate the impact of the addition of aggregates, such as quartz powder, the binder to aggregate ratio was varied from 100:0 to 20:80, referring to the metakaolin to quartz powder ratio.

The major conclusions derived from the experimental study can be summarized as follows:

- A higher water content of the geopolymer mixture leads to a better workability, as indicated by the increase in flow spread of the fresh mortar, from 190 mm for GP-Ref to over 300 mm for GP_150. This enhanced workability is also indicated by the increase of relative flow spread from 2.6 for GP_Ref to 8.0 for GP_150. Simultaneously, the compressive strengths of the mortar specimens decreased, from 54.3 MPa for GP_Ref to 29.1 MPa for GP_150, due to an increase in capillary porosity. Simultaneously, the flexural strength declined from 4.4 MPa GP_Ref to 4.0 MPa for GP_150 as the water content increased. At the same time, the increasing water content led to an improved deaeration effect and therefore a low air void content, as indicated by micro X-ray computer tomography.
- The binder to aggregate ratio is crucial for the compressive and flexural strengths of the mortar specimens. Through the addition of quartz powder up to a ratio of 20:80 of metakaolin to quartz, an increase in strength can be witnessed. The compressive strength of the geopolymer obtained without any quartz powder amounted to 46.55 MPa, and its strength can be increased to 81.43 MPa in the case of the 20:80 mixture of metakaolin and quartz. Simultaneously, the flexural strength increased. This finding gives new information for the optimal design of the geopolymer mixture.
- The geopolymer formation is a complex process, which requires a detailed knowledge of the underlying factors that can influence the fresh mortar properties as well as the mechanical properties of the final geopolymer mortars.

Supplementary Materials: The following supporting information can be downloaded at: https://www.mdpi.com/article/10.3390/min14080823/s1. Figure S1: Powder X-ray diffractogram of the metakaolin Metamax®. Figure S2: Powder X-ray diffractogram of the quartz powder MILLISIL W3®. Figure S3: Pore size distributions according to incident light microscopy. Figure S4: Nitrogen sorption isotherm for GP_Ref recorded at 77 K. Figure S5: Pore size distribution according to the BJH method on the basis of the desorption data. Figure S6: Results of the mercury intrusion porosimetry of the whole pore diameter area (3.5–100,000 nm). Figure S7: Powder X-ray diffractograms of GP_Ref and GP_150. Table S1: Overview of the mechanical properties of the mortar specimens. Table S2: Molar ratios of the mixing design.

Author Contributions: Conceptualization: F.D. (Felix Dathe), A.K., F.D. (Frank Dehn), writing—original draft—review, editing: F.D. (Felix Dathe), A.K. and F.D. (Frank Dehn), writing—original draft preparation—review, editing: F.D. (Felix Dathe), A.K. and F.D. (Frank Dehn), measurements: F.D. (Felix Dathe), S.O. and A.K.; analysis: A.K., visualization, F.D. (Felix Dathe), S.O. and A.K., supervision: A.K. and F.D. (Frank Dehn). All authors have read and agreed to the published version of the manuscript.

Funding: Parts of this project were funded by the German Research Foundation (DFG) (From common clay to geopolymer binder—fundamental crystallographic and structural engineering investigations, 325967999).

Data Availability Statement: The original contributions presented in the study are included in the article/supplementary material, further inquiries can be directed to the corresponding author.

Acknowledgments: The authors would like to thank Florian Fuchs for the μXCT imaging and the Workgroup of Dirk Enke for performing individual MIP measurements, both from the University of Leipzig.

Conflicts of Interest: The authors declare that they have no known competing financial interests or personal relationships that could have appeared to influence the work reported in this paper.

References

1. International Energy Agency, Glob. Status Report: Towards a Zero-Emission, Efficient and Resilient Buildings and Construction Sector. 2018. Available online: https://www.iea.org/reports/2018-global-status-report (accessed on 4 June 2024).
2. Petek Gursel, A.; Masanet, E.; Horvath, A.; Stadel, A. Life-cycle inventory analysis of concrete production: A critical review. *Cem. Concr. Compos.* **2014**, *51*, 38–48. [CrossRef]
3. Habert, G.; Miller, S.A.; John, V.M.; Provis, J.L.; Favier, A.; Horvarth, A.; Scrivener, K.L. Environmental impacts and decorbonization strategies in the cement and concrete industries. *Nat. Rev. Earth Environ.* **2020**, *1*, 559–573. [CrossRef]
4. Farooq, F.; Jin, X.; Faisal Javed, M.; Akbar, A.; Izhar Shah, M.; Aslam, F.; Alyousef, R. Geopolymer concrete as sustainable material: A state of the art review. *Constr. Build. Mater.* **2021**, *306*, 124762. [CrossRef]
5. Davidovits, J. Geopolymers: Man-Made Rock Geosynthesis and the Resulting Development of Very Early High Strength Cement. *J. Mater. Educ.* **1994**, *16*, 91–139.
6. Davidovits, J. Geopolymers: Inorganic polymeric new materials. *J. Therm. Anal. Calorim.* **2005**, *37*, 1633–1656. [CrossRef]
7. Palomo, A.; Grutzeck, M.W.; Blanco, M.T. Alkali-activated fly ashes: A cement for the future. *Cem. Concr. Res.* **1999**, *29*, 1323–1329. [CrossRef]
8. Provis, J.L.; van Deventer, J.S.J. (Eds.) *Geopolymers: Structures, Processing, Properties and Industrial Applications*; CRD Press: Boca Raton, FL, USA; Woodhead Publ.: Cambridge, UK, 2019.
9. He, C.; Osbaeck, B.; Makovicky, E. Pozzolanic reactions of six principal clay minerals: Activation, reactivity assessments and technological effects. *Cem. Concr. Res.* **1995**, *25*, 1691–1702. [CrossRef]
10. Seiffarth, T.; Hohmann, M.; Posern, K.; Kaps, C. Effect of thermal pre-treatment conditions of common clays on the performance of clay-based geopolymeric binders. *Appl. Clay Sci.* **2013**, *73*, 35–41. [CrossRef]
11. Dathe, F.; Strelnikova, V.; Werling, N.; Emmerich, K.; Dehn, F. Influence of lime, calcium silicate and portlandite on alkali activation of calcined common clays. *Open Ceram.* **2021**, *7*, 100152. [CrossRef]
12. Liew, Y.M.; Heah, C.Y.; Mohd Mustafa, A.B.; Kamarudin, H. Structure and properties of clay-based geopolymer cements: A review. *Prog. Mater. Sci.* **2016**, *83*, 595–629. [CrossRef]
13. Werling, N.; Schwaiger, R.; Dathe, F.; Dehn, F.; Emmerich, K. Micromechanical properties of geopolymers with different calcined clay precursors. *Appl. Clay Sci.* **2024**, *250*, 107259. [CrossRef]
14. Patankar, S.V.; Jamkar, S.S.; Ghugal, Y.M. Effect of water-to-geopolymer binder ratio on the production of fly ash based geopolymer conctrete. *Int. J. Adv. Technol. Civ. Eng.* **2012**, *1*, 296–300. [CrossRef]
15. Luhar, S.; Nicolaides, D.; Luhar, I. Fire Resistance Behaviour of Geopolymer Concrete: An Overview. *Buildings* **2021**, *11*, 82. [CrossRef]
16. Koenig, A.; Herrmann, A.; Overmann, S.; Dehn, F. Resistance of alkali-activated binders to organic acid attack: Assessment of evaluation criteria and damage mechanisms. *Constr. Build. Mater.* **2017**, *151*, 405–413. [CrossRef]
17. Bakharev, T. Durability of geopolymer materials in sodium and magnesium sulfate solutions. *Cem. Concr. Res.* **2005**, *35*, 1233–1246. [CrossRef]
18. Albidah, A.; Alghannam, M.; Abbas, H.; Almusallam, T.; Al-Salloum, Y. Characteristics of metakaolin-based geopolymer concrete for different mix design parameters. *J. Mater. Res. Technol.* **2021**, *10*, 84–98. [CrossRef]
19. Pulidori, E.; Pelosi, C.; Fugazzotto, M.; Pizzimenti, S.; Carosi, M.R.; Bernazzani, L.; Stroscio, A.; Tiné, M.R.; Mazzoleni, P.; Barone, G.; et al. Thermal behavior of Sicilian clay-based geopolymers. *J. Therm. Anal. Calorim.* **2024**, *23*, 1–13. [CrossRef]
20. Dal Poggetto, G.; Kittisayarm, P.; Pintasiri, S.; Chiyasak, P.; Leonelli, C.; Chaysuwan, D. Chemical and Mechanical Properties of Metakaolin-Based Geopolymers with Waste Corundum Powder Resulting from Erosion Testing. *Polymers* **2022**, *14*, 5091. [CrossRef] [PubMed]
21. D'Angelo, A.; Dal Poggetto, G.; Piccolella, S.; Leonelli, C.; Catauro, M. Characterisation of White Metakaolin-Based Geopolymers Doped with Synthetic Organic Dyes. *Polymers* **2022**, *14*, 3380. [CrossRef]
22. Zuhua, Z.; Xiao, Y.; Huajun, Z.; Yue, C. Role of water in the synthesis of calcined kaolin-based geopolymer. *Appl. Clay Sci.* **2009**, *43*, 218–223. [CrossRef]
23. Yao, X.; Zhang, Z.; Zhu, H.; Chen, Y. Geopolymerization process of alkali–metakaolinite characterized by isothermal calorimetry. *Thermochim. Acta* **2009**, *493*, 49–54. [CrossRef]
24. Davidovits, J. *Geopolymer Chemistry and Applications*, 5th ed.; Geopolymer Institute: Saint-Quentin, France, 2020.
25. Van Jaarsveld, J.G.S.; Van Deventer, J.S.J.; Lukey, G.C. The effect of composition and temperature on the properties offly ash- and kaolinite-based geopolymers. *Chem. Eng. J.* **2002**, *89*, 63–73. [CrossRef]
26. *EN 196-1:2016*; Methods of Testing Cement—Part 1, Determination of Strength. European Committee for Standardization: Brussels, Belgium, 2016.
27. *EN 480-11:2005*; Admixtures for Concrete, Mortar and Grout—Test Methods—Part 11: Determination of Air Void Characteristics in Hardened Concrete. European Committee for Standardization: Brussels, Belgium, 2005.
28. Koenig, A. Analysis of air voids in cementitious materials using micro X-ray computed tomography (μXCT). *Constr. Build. Mater.* **2020**, *244*, 118313. [CrossRef]
29. *EN 1015-3:2007*; Methods of Test for Mortar for Masonry—Part 3: Determination of Consistence of Fresh Mortar (by Flow Table). European Committee for Standardization: Brussels, Belgium, 2007.

30. Wang, H.; Li, H.; Yan, F. Synthesis and mechanical properties of metakaolinite-based geopolymer. *Colloids Surf. A Physicochem. Eng. Asp.* **2005**, *268*, 1–6. [CrossRef]
31. Yunsheng, Z.; Wei, S.; Zongjin, L. Composition design and microstructural characterization of calcined kaolin-based geopolymer cement. *Appl. Clay Sci.* **2010**, *47*, 271–275. [CrossRef]
32. Muller, A.C.A.; Scrivener, K.L. A reassessment of mercury intrusion porosimetry by comparison with 1H NMR relaxometry. *Cem. Concr. Res.* **2017**, *100*, 350–360. [CrossRef]
33. Pelosi, C.; Occhipinti, R.; Finocchiaro, C.; Lanzafame, G.; Pulidori, E.; Lezzerini, M.; Barone, G.; Mazzoleni, P.; Rosaria Tiné, M. Thermal and morphological investigations of alkali activated materials based on Sicilian volcanic precursors. *Mater. Lett.* **2023**, *335*, 133773. [CrossRef]
34. Kasaniya, M.; Thomas, M.D.A.; Moffatt, T.; Hossack, A. Microstructure and microanalysis of portland cement pastes with high *w/c* ratios. *Cem. Concr. Res.* **2024**, *183*, 107575. [CrossRef]
35. Dujardin, N.; Salem, T.; Feuillet, V.; Fois, M.; Ibos, L.; Poilane, C.; Manuel, R. Measurement of pore size distribution of building materials by thermal method. *Constr. Build. Mater.* **2020**, *245*, 118417. [CrossRef]
36. Abell, A.B.; Willis, K.L.; Lange, D.A. Mercury Intrusion Porosimetry and Image Analysis of Cement-Based Materials. *J. Colloid Interface Sci.* **1999**, *211*, 39–44. [CrossRef]
37. Kang, S.H.; Jeong, Y.; Tan, K.H.; Moon, J. The use of limestone to replace physical filler of quartz powder in UHPFRC. *Cem. Concr. Compos.* **2018**, *94*, 238–247. [CrossRef]
38. Haruna, S.; Mohammed, B.S.; Wahab, M.M.A.; Al-Fakih, A. Effect of aggregate-binder proportion and curing technique on the strength and water absorption of fly ash-based one-part geopolymer mortars. *IOP Conf. Ser. Mater. Sci. Eng.* **2021**, *1101*, 01202. [CrossRef]
39. Joseph, B.G.; Mathew, G. Influence of aggregate content on the behavior of fly ash based geopolymer concrete. *Sci. Iran.* **2012**, *19*, 1188–1194. [CrossRef]
40. Arellano-Aguilar, R.; Burciaga-Díaz, O.; Gorokhovsky, A.; Escalante-García, J.I. Geopolymer mortars based on a low grade metakaolin: Effects of the chemical composition, temperature and aggregate: Binder ratio. *Constr. Build. Mater.* **2014**, *50*, 642–648. [CrossRef]